Electrical Semiconductivity of Stacked Layer Coordination Polymers of Rhodium(I)

IRENE FEINSTEIN-JAFFE*† and AVI EFRATY‡

Department of Organic Chemistry, The Weizmann Institute of Science, Rehovot, Israel 76100. *Received January 9, 1986*

A study directed at the molecular design and preparation of unconventional coordination polymers with "tailor-made" chemical and/or physical properties yielded some novel tetragonal rhodium(I) polymers of the general type [Rh(aryl diisocyanide)$_2$$^+Cl^-$]$_n$.[1-5] A powder X-ray diffractometric trace analysis of these polymers revealed a stacked layer structure with an extensive network of columnar metal chains. A schematic representation of the three-dimensional structure of some coordination polymers of rhodium(I) with stereochemically rigid collinear linkages is shown in Figure 1. Further support for the presence of columnar metal chains in these polymers was obtained from their electronic spectra.[1,4] In view of the foregoing, it was considered of interest to examine the electrical conductivity of the polymers, a study reported herein.

Experimental Section

The [Rh(aryl diisocyanide)$_2$$^+Cl^-$]$_n$ polymers were prepared from [Rh(CO)$_2$Cl]$_2$ and the respective aryl diisocyanide ligands as previously reported.[1-5] The conductivity experiments described here were conducted on compressed-powder pellets (20 ton min^{-1} cm^{-2}) by the two-electrode method[6] (ac, 1 kHz) using a laboratory-designed holder apparatus and a 1680A digital automatic capacitance bridge assembly (General Radio Co., Concord, MA).

Results and Discussion

The room temperature (~25 °C) conductivities of these polymers (1.65×10^{-4} to 4.00×10^{-6} Ω^{-1} cm^{-1}) (see Table I) were found to be considerably higher than those reported for either Rh(CO$_2$)(acac) (10^{-11} Ω^{-1} cm^{-1}; E = 0.32–0.44 eV; Rh(I)–Rh(I), 3.26 Å)[7] or [Rh$_2$(CNPh)$_8$](BPh$_4$)$_2$ [7.2×10^{-11} Ω^{-1} cm^{-1}; Rh(I)–Rh(I), 3.19 Å].[8] Room temperature (25 °C) measurements conducted on a series of (alkyl and aryl isocyanide)rhodium(I) cations with TCNQ$^{\bullet-}$ as a radical anion, [Rh(CNR)$_4$]$^+$TCNQ$^{\bullet-}$[9] and [Rh(CNR)$_4$]$^+$(TCNQ)$_2$$^{\bullet-}$ showed these materials to have conductivities in the range 10^{-3} to $>10^{-10}$ Ω^{-1} cm^{-1}. In the temperature range 20–90 °C these complexes behave as typical semiconductors with activation energies of 0.065–0.55 eV.[9] A very recent report[10] on the oxidized Rh(III) systems, [Rh(RNC)$_4$I$_2$]$^+$-TCNQ$^{\bullet-}$ reveals room temperature (25 °C) conductivities in the range 10^{-3} to 10^{-6} Ω^{-1} cm^{-1} and for the complex salts [Rh(C$_6$H$_5$NC)$_4$I$_2$]$^+$(TCNQ)$_2$$^{\bullet-}$ and [Rh(4-MeC$_6$H$_4$NC)$_4$I$_2$]$^+$(TCNQ)$_2$$^{\bullet-}$, 8.3 Ω^{-1} cm^{-1} and 30 Ω^{-1} cm^{-1}, respectively. Activation energies for these latter systems, calculated in the temperature range 30–85 °C, are 0.043–0.39 eV. Additional higher conductivities were encountered for a series of cationic rhodium complexes[8] of the types [Rh(CNCH$_3$)$_4$]$^+$X$^-$ [X = Cl (3.3×10^{-2} Ω^{-1} cm^{-1}), BF$_4$ (2.2×10^{-2} Ω^{-1} cm^{-1})], [Rh(CNCH$_2$CH$_3$)$_4$]$^+$X$^-$ [X = Cl (6.7×10^{-4} Ω^{-1} cm^{-1}), ClO$_4$ (5.1×10^{-4} Ω^{-1} cm^{-1}), and PF$_6$ (3.9×10^{-5} Ω^{-1} cm^{-1})], and [Rh(CNCHCH$_2$)$_4$]$^+$X$^-$ [X = Cl (2.9×10^{-4} Ω^{-1} cm^{-1}), ClO$_4$ (5.6×10^{-3} Ω^{-1} cm^{-1}), and PF$_6$ (5.6×10^{-4} Ω^{-1} cm^{-1})] which contain Rh–Rh distances in the range 2.94–2.96 Å.

The conductivity of the compressed-powder pellets of the polymers with 1,4-diisocyanobenzene and 4,4′-diisocyanobiphenyl linkages was measured in the temperature range 25–150 °C. Thermal gravimetric analyses on these polymers[4] has shown decomposition to occur above 400 °C; therefore the temperature range chosen for conductivity measurements is an appropriate one. The results of the temperature-dependent conductivity study, expressed in the form of ln resistivity (ρ, Ω-cm) vs. $10^3/T$ [K^{-1}], are shown in Figure 2. Noteworthy are the nearly linear plots which allow the calculation of the respective band-gap energies according to the equation $\sigma = \sigma_0 \exp(-E/2kT)$, where σ (=$1/\rho$) stands for conductivity (Ω^{-1} cm^{-1}), and k and T stand for Boltzmann's constant (8.62×10^{-5} eV/deg) and absolute temperature (K), respectively. The calculated band-gap energies for the polymers with the 1,4-diisocyanobenzene [0.47 eV] and 4,4′-diisocyanobiphenyl [0.25 eV] linkages were obtained by accounting for all of the points along the respective plots (Figure 2). All conductivity measurements were conducted with ac techniques, and therefore the probability of interparticle contacts dominating the conductivity data is lessened.

The lower resistivity (ρ) and higher conductivity (σ) found for the 1,4-diisocyanobenzene rather than for the 4,4′-diisocyanobiphenyl polymer are consistent with the presence of a somewhat shorter (~0.1 Å) Rh(I)–Rh(I) bond distance in the former. The low resistivity and relatively high energy band gap found for the 1,4-diisocyanobenzene polymer may suggest that the conductivity in this system depends on additional factors apart from intermetallic interactions. In this regard, noteworthy are the orthogonal

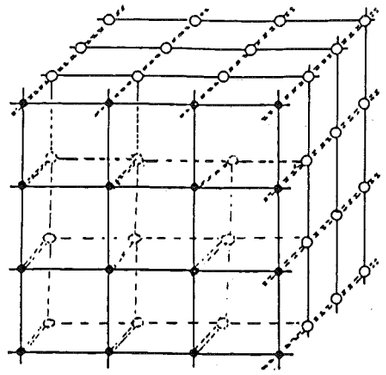

Figure 1. Schematic representation of the three-dimensional [Rh(diisocyanide)$_2$]$_2$ network in tetragonal coordination polymers of the type [Rh(diisocyanide)$_2$$^+Cl^-$]$_n$ with the collinear linkages (—) 1,4-diisocyanobenzene and 4,4′-diisocyanobiphenyl and columnar metal chains (– – –).

Table I
Electrical Conductivity Measurements of [Rh(aryl diisocyanide)$_2$$^+Cl^-$]$_n$ Polymers

aryl diisocyanide ligand	pellet thickness,[a] mm	Rh–Rh distance,[b] Å	measd conductivity, Ω^{-1}	specific conductivity, Ω^{-1} cm^{-1}
1,4-diisocyanobenzene	0.20	3.31	3.3×10^{-6}	1.65×10^{-4}
4,4′-diisocyanobiphenyl	0.50	3.40	6.1×10^{-7}	1.22×10^{-5}
1,3-diisocyanobenzene	0.20	[c]	8.0×10^{-8}	4.00×10^{-6}
4,4′-diisocyanodiphenylmethane	0.20	3.36	4.0×10^{-7}	2.00×10^{-5}
1,5-diisocyanonaphthalene	0.35	3.41	1.1×10^{-7}	3.14×10^{-6}

[a] Compressed powder pellets prepared under 20 ton cm^{-2} min^{-1}. Variation ±0.05 mm. [b] Bond distance data are those quoted in ref 4, a full manuscript submitted. [c] Not determined.

† Department of Materials Research, Weizmann Institute of Science, Rehovot, Israel 76100.
‡ Assaf Pharmaceutical Industries Ltd., subsidary of SUMMA Medical Corp. USA., Jerusalem, Israel.

0024-9297/86/2219-2076$01.50/0

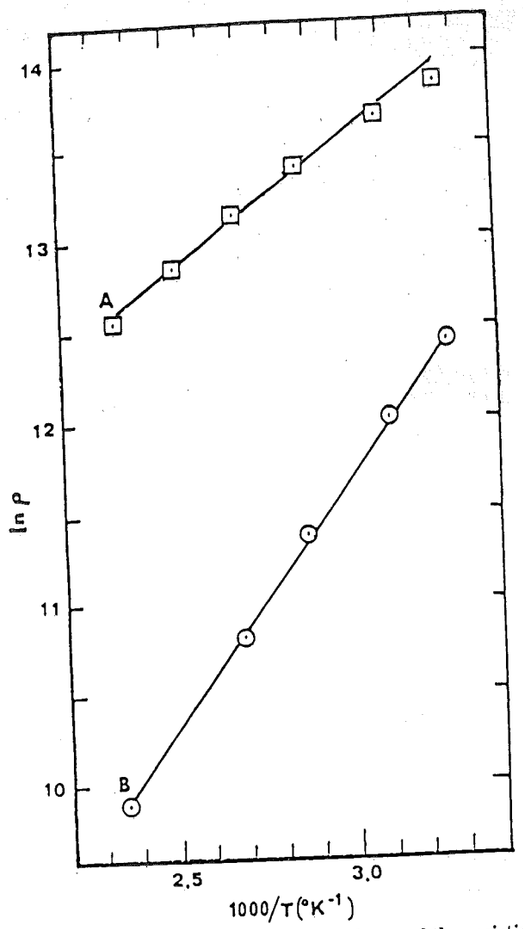

Figure 2. Temperature ($10^3/T$) dependence of the resistivity (ln ρ; Ω·cm) measured on compressed powder pellets of [Rh(4,4-diisocyanobenzene)$_2$$^+Cl^-$]$_n$ (A) and [Rh(1,4′-diisocyanobiphenyl)$_2$$^+Cl^-$]$_n$ (B).

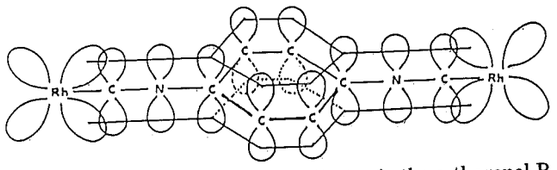

Figure 3. Transfer of electronic effects via the orthogonal P$_\pi$ orbitals of the collinear 1,4-diisocyanobenzene linkage.

P$_\pi$ orbitals of the 1,4-diisocyanobenzene linkages (Figure 3) which should allow the transfer of electronic effects in the two-dimensional layers (100 planes) of this polymer. A similar process in the case of the terminally coordinated 4,4′-diisocyanobiphenyl linkage would be either restricted or forbidden, depending on the dihedral angle of the phenylene rings of the biphenylene unit. The overall conductivity (σ) of these polymers should include intraplanar as well as interplanar contributions; the latter should be larger for the polymer with the 1,4-diisocyanobenzene linkages than for the 4,4′-diisocyanobiphenyl polymer. Anisotropic electrical properties may be determined by the study of single crystals. Unfortunately, the polymers under review have not yet been obtained in suitable crystallinic form to allow for such study.

The oxidation states of many of the cationic rhodium tetrakis(monoisocyanide) systems have been found to be greater than one (1.0–1.25).[8] This data may then suggest that these systems are one-dimensional metals in which the metallic behavior has been quenched by crystalline disorder and imperfections. On the other hand, the possibility of either a small band-gap intrinsic or extrinsic semiconductor systems, with the latter being dominated by Rh(II) "impurities", was also considered for these complexes.[8] Similar considerations may also apply to the coordination polymers reported herein.

Registry No. [Rh(1,4-diisocyanobenzene)$_2$$^+Cl^-$]$_2$, 74620-93-2; [Rh(4,4′-diisocyanobiphenyl)$_2$$^+Cl^-$]$_n$, 74620-95-4.

References and Notes

(1) Efraty, A.; Feinstein, I.; Frolow, F.; Wackerle, L. *J. Am. Chem. Soc.* **1980**, *102*, 6341.
(2) Efraty, A.; Feinstein, I.; Wackerle, L.; Frolow, F. *Angew. Chem., Intl. Ed. Engl.* **1980**, *19*, 633.
(3) Efraty, A.; Feinstein, I.; Frolow, F.; Goldman, A. J. *J. Chem. Soc., Chem. Commun.* **1980**, 864.
(4) Feinstein-Jaffe, I.; Efraty, A.; Frolow, F.; Wackerle, L.; Goldman, A., submitted.
(5) Efraty, A.; Feinstein, I.; Frolow, F. *Inorg. Chem.* **1982**, *21*, 485.
(6) Gutmann, F.; Lyons, L. E. *Organic Semiconductors*; Wiley: New York, 1967; pp 44–47.
(7) Collman, J. P.; Slirkin, L.; Ballard, L. F.; Monleith, L. K.; Pitt, C. G. In *International Symposium on Decomposition of Organometallic Compounds to Refractory Ceramics, Metals and Metal Alloys*; Mazdiyashi, K. S., Ed.; University of Dayton Research Institute: Dayton, OH, 1968; p 269. Monleith, L. K.; Ballard, L. F.; Pitt, C. G. *Solid State Commun.* **1968**, *6*, 301.
(8) Gordon, J. G., II; Williams, R.; Hsu, C.-H.; Cuellar, E.; Samson, S.; Mann, K.; Gray, H. B.; Hadek, U.; Somoano, R. *Ann. N.Y. Acad. Sci.* **1978**, *313*, 58.
(9) Iinuma, T.; Tanaka, T. *Inorg. Chim. Acta* **1981**, *49*, 79.
(10) Yashi, G.-E. M.; Iinuma, T.; Tanaka, T. *Inorg. Chim. Acta* **1985**, *102*, 145.

Molecular Design of Multicomponent Polymer Systems. 8. New Acrylonitrile–Butadiene–Styrene-like Resins from Styrene–Acrylonitrile-Based Mechanical Blends

R. FAYT and PH. TEYSSIÉ*

Laboratory of Macromolecular Chemistry and Organic Catalysis, University of Liège, Sart-Tilman (B6), 4000 Liège, Belgium. *Received July 8, 1985*

One of the main applications of polymer blends is in the manufacture of impact-resistant materials, since phase separation is an essential feature for the rubber toughening of brittle plastics. In acrylonitrile–butadiene–styrene (ABS) resins, the rubbery phase usually consists of polybutadiene, nitrile rubber, or poly(styrene-*co*-butadiene) rubber (SBR). The largest part of the resins now manufactured is prepared by a graft copolymerization process of styrene and acrylonitrile in the presence of a preformed rubber.[1] Although mechanical blending remains certainly a very attractive and more versatile way toward these polyblends, it has important deficiencies that cause it to be less efficient than the copolymerization techniques. Among the necessary features of the rubber phase, good adhesion to the matrix, adequate cross-linking, and average particle diameter near the optimum value (ca. 0.5 μm) are the most important ones to achieve high impact performances.[2] These requirements are not met when melt blending styrene–acrylonitrile (SAN) with a commercial rubber. In order to alleviate that situation, we have investigated combinations of commercial thermoplastic elastomers in a SAN matrix, more precisely styrene–butadiene block copolymers (SBS) and appropriate polymeric

0024-9297/86/2219-2077$01.50/0

Table I
Molecular Characteristics of PS–PMMA and PB–PMMA Copolymers (50/50 Composition)

sample code	block copolymer	$M_{n\,tot}$
SMA 32	PS–PMMA	220 000
SMA 33	PS–PMMA	150 000
BMA 11	PB–PMMA	140 000
BMA 20	PB–PMMA	200 000
BMA 29 and 35	PB–PMMA	470 000–130 000 (2 GPC peaks)

emulsifiers. The use of a SBS copolymer as the rubber phase has the advantage of overcoming the difficulty to control proper cross-linking during the blending process since such a material is physically cross-linked thanks to formation of PS microdomains. Furthermore, it is now recognized that both phase dispersion and interfacial adhesion in incompatible polymer blends can be provided by well-chosen diblock copolymers: we have indeed largely demonstrated the validity and applicability of that concept in the melt blending of many model polymer mixtures, some of them being already published.[3-5] In the present case, the adhesion between the SBS rubber phase and the SAN matrix could be provided either by a poly(styrene-*block*-methyl methacrylate) PS–PMMA or a poly(butadiene-*block*-methyl methacrylate) PB–PMMA diblock copolymer. Thanks to good mutual interactions, copolymers having a syndiotactic PMMA block act as efficient emulsifiers for SAN-based blends.[6] Furthermore, since SBS displays PS and PB domains, its anchoring into the SAN matrix can be ensured by using either a PS or a PB block, provided solubilization of the corresponding blocks occurs in each case; we were therefore also interested in the comparison of both situations.

Experimental Section

Results presented here were obtained with a SAN resin (from Labofina S.A): SAN K 17 (27% AN). The thermoplastic elastomer was Solprene 411 from Phillips (four-arm star-shaped block copolymer, 30% PS, $\bar{M}_n$ 280 000). PS–PMMA and PB–PMMA diblock copolymers were synthesized in the laboratory by anionic copolymerization techniques. For PS–PMMA, styrene was polymerized in pure THF at −78 °C for 30 min (*sec*-BuLi/α-methylstyrene mixtures as initiator).[7] Pure MMA was then introduced in the reaction medium and allowed to polymerize for 2 h at −78 °C. PB–PMMA copolymers were prepared as follows: Butadiene was polymerized in benzene at 40 °C for 12 h (*sec*-BuLi initiation). THF was then added to the medium progressively cooled to −78 °C. (THF/Bz = 5), and the polybutadienyl anion was end-capped with a few 4-vinylpyridine units in order to generate a less reactive terminal anion. MMA was added and allowed to polymerize at −78 °C for 2 h. Table I summarizes the characteristics of the block copolymers used.

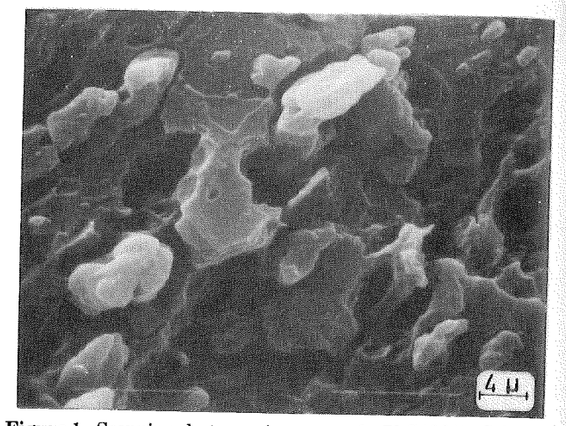

Figure 1. Scanning electron microscopy of a 70 SAN/30 Solprene 411 blend (fracture surface from a Charpy impact test).

Blends were prepared on a laboratory two-roll mill at 200 °C. SAN was first molten on the roll mill before the successive incorporation of Solprene and the emulsifier. The three components were then mixed at 30 rpm for 5 min. The samples were compression molded at 200 °C for 3 min (2500 psi) into sheets from which tensile and impact specimens were machined.

Results and Discussion

First screening experiments demonstrated that when a SAN resin is melt blended with an un-cross-linked rubber (polybutadiene), on a laboratory two-roll mill, lamination occurs, even at low rubber content; that phenomenon does not take place when a thermoplastic elastomer (SBS copolymer) is used. This observation demonstrates the benefit of using a physically cross-linked elastomer to design new ABS's by melt blending.

Pure blends of SAN with SBS Solprene 411 (star-shaped copolymer) do not exhibit good tensile and impact properties even when the rubber content is high (±30%), as observed in Table II. Fracture surface examination by scanning electron microscopy put in evidence coarse dispersions of the phases, and lack of adhesion between them (Figure 1). That situation is alleviated when the blends are modified with a block copolymer PS–PMMA. Results in Table II show that the modified blends exhibit a higher ductibility (ϵ_B) and impact resistance (Charpy impact strength) than pure blends. However, these performances remain lower than those of a commercial high-impact ABS resin (Cycolac GSM from Borg Warner), taken as reference.

Table II
Tensile and Impact Behavior of Some SAN/Solprene 411 Blends[a]

SAN, %	Solprene 411, %	copolymer, %	% total rubber[b]	E, MPa	σy, MPa	σ_B, MPa	ϵ_B, %	Charpy, kJ/m^2	Izod, ft·lb/in.	F.D. (Gardner), in.·lb
100				2000		66	6	3.5		
70	30		30	1230		33.2	7.2	6.8		
66.5	28.5	5 SMA32	28.5	1310		34.5	13.6	10.9		
71.4	23.8	4.7 SMA33	23.8	1460	39.5	38.5	16.4	12.4		
65.6	27.3	9.2 SMA33	27.3	1710	39.7	38.9	14.5	11.9		
72.7	18.1	9.2 BMA11	22.7					21.6	5.88	120
63.6	27.3	9.1 BMA11	31.8					18.9		
72.7	18.1	9.2 BMA20	22.7	1640	39.7	33.5	23.5	16.8	7.46	140
66.5	23.5	10 BMA20	28.5	1590	35.9	29.9	23.4	31.8	8.51	140
72.7	18.1	9.2 BMA29	22.7			30.9	21.8	35.2		
72.7	18.1	9.2 BMA35	22.7	1590	35.3			33.9		
	ABS[c]		30	1490	43.5	34	19	19.1	5.48	120

[a] Tensile tests, were performed on specimens DIN 53448 at a cross-head speed of 2 cm·min^{-1}. Charpy impact tests, were performed on specimens DIN 53453 (0.3-mm notch). [b] Percent total rubber includes the PB block of the PB–PMMA copolymer. [c] Cycolac GSM natural.

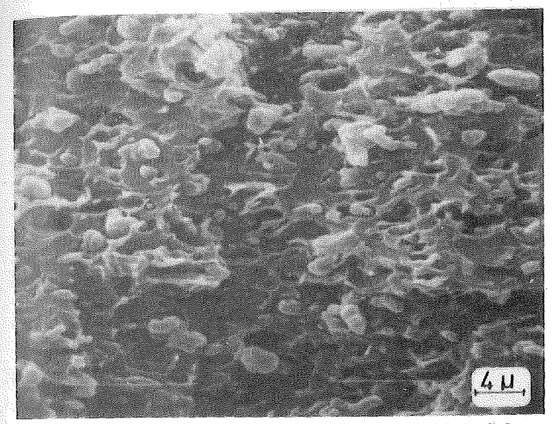

Figure 2. Scanning electron microscopy of a 70 SAN/24 Solprene 411/6 copolymer PS–PMMA blend (fracture surface from a Charpy impact test).

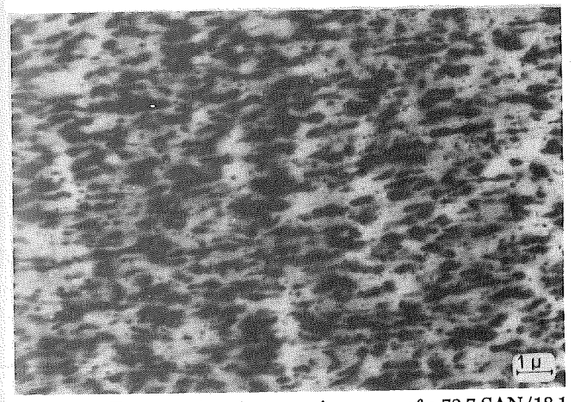

Figure 3. Transmission electron microscopy of a 72.7 SAN/18.1 Solprene 411/9.2 copolymer PB–PMMA blend (PB phases were stained with osmium tetraoxide).

Micrographs also demonstrate that, while the particle size is significantly decreased upon the addition of the block copolymer, the adhesion between the rubber phase and the SAN matrix is still limited; furthermore, the fracture of the blends remains brittle and controlled by crazing only (Figure 2).

Such limitations are no longer observed when SAN/SBS blends are emulsified with PB–PMMA diblock copolymer. Table II shows that impact performances significantly higher than that of the commercial ABS can be obtained even at lower rubber content (22.7% rubber phase in comparison with 30% in Cycolac). Izod impact tests as well as falling dart test performed on selected samples confirm that superiority.

Microscopy observations put in evidence the beneficial effect of PB–PMMA copolymers in SAN/SBS blends. The state of dispersion was more precisely evidenced on transmission electron micrographs, after staining the rubber phase with osmium tetraoxide. Figure 3 shows that the rubber particle size is generally less than 1 μm and is thus near the optimum reported value for a "classical" ABS resin. Although some distortion could result from the knife compression in the ultramicrotome, it is apparent that these rubber particles are not spherical but irregularly elongated. The particle shape seems therefore not to be such a critical parameter in controlling the impact performances of SAN/SBS blends. Furthermore, scanning electron microscopy examination of fracture surfaces puts in evidence a strong adhesion between the phases. In fact, these phases are so intimately anchored to each other that it is not possible to distinguish them (Figure 4). On the other hand, the fracture surface of the ABS resin (Figure 5) exhibits holes that could be attributed to rubber particles expelled during the fracture; such holes are not observed in our blends, where fracture seems to occur without interfacial decohesion.

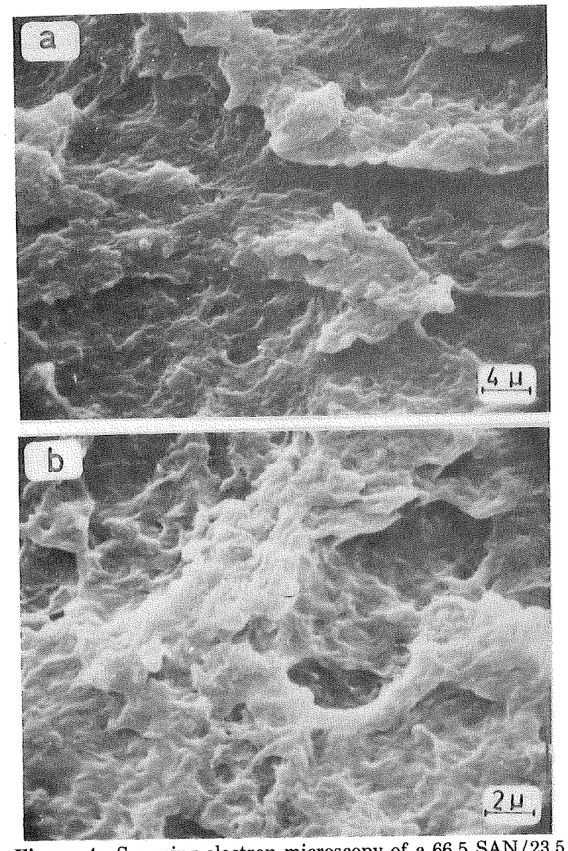

Figure 4. Scanning electron microscopy of a 66.5 SAN/23.5 Solprene 411/10 PB–PMMA copolymer blend (fracture surface from a Charpy impact test).

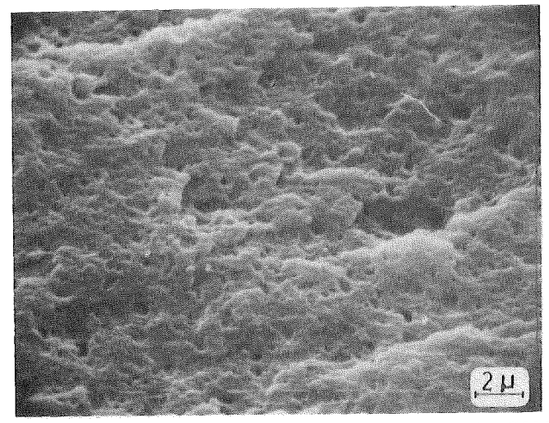

Figure 5. Scanning electron microscopy of ABS Cycolac GSM. (Fracture surface from a Charpy impact test).

In other words, interfacial adhesion seems to be stronger in our blends than in the commercial resin. These results demonstrate further that adhesion between rubber par-

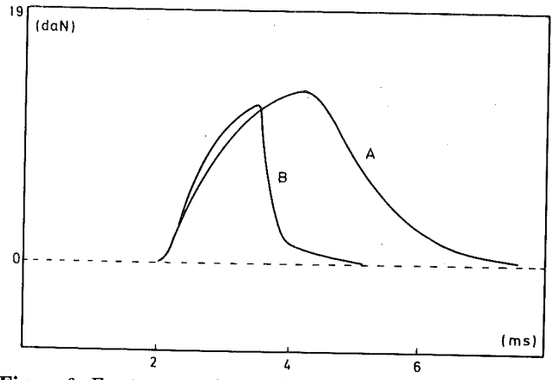

Figure 6. Fractograms of a 66.5 SAN/23.5 Solprene 411/10 copo PB–PMMA blend (curve A) and of ABS Cycolac GSM (curve B). Charpy impact tests on notched specimens DIN 53453.

ticles and the matrix is a very important parameter to impart high-impact performances to toughened resins and also that such an adhesion can be provided by using a suitable polymeric emulsifier.

These scanning electron micrographs also demonstrate that the emulsified SAN/SBS blends mainly deform by shear; this response is even more pronounced in our blends than in the commercial ABS. Fractograms confirm that situation; Figure 6 shows indeed that fracture of our blends (A) is much more ductile than that of commercial ABS (B): a definitely higher energy for fracture propagation is indeed recorded for the former, and that possibility to modify the *profile* of the impact response is particularly appealing.

Finally, it is interesting to note that such high-level performances are not detrimental to the Young's modulus of the materials. Values listed in Table II demonstrate that the modulus of our blends is generally higher than that of the commercial ABS and in fact rather close to pure rigid SAN.

When the behavior of PS–PMMA and PB–PMMA copolymers is compared, it can be concluded that a PB block solubilizes more easily in the PB domains of the SBS rubber phase than can a PS block into the corresponding PS domains. That situation was expected considering that, in SBS, PS forms discrete domains in a PB matrix, which therefore is more accessible to the PB blocks of the emulsifier. The effect of the molecular characteristics of these emulsifiers should of course be investigated more deeply.

Nevertheless, the present results, although not fully optimized, demonstrate unambiguously that very high-impact performances can be obtained by simple melt blending a SAN resin with a suitable rubber and an emulsifier such as PB–PMMA copolymer. More systematic experiments are in progress in order to evaluate more precisely the behavior of these materials with respect to the characteristics of the two block copolymers (rubber phase and emulsifier) and composition.

With respect to the technological significance of these results, it is clear that performances of our blends should be optimized as injection-molding materials like the commercially produced ABS are designed. Particular attention should therefore be paid to flow properties, since the present material exhibits a melt viscosity too high for an injection process. Furthermore, optimized commercial ABS resins exhibit a two-phase structure well stabilized against delamination under high shear. It is assumed that our blends behave similarly thanks to the strong interfacial adhesion that has been evidenced.[9] Nevertheless, morphology and impact properties of injection-molded materials should be evaluated in order to define their real performance level in comparison with classical ABS. Generally speaking, however, the powerfulness of this "blends molecular engineering" concept is once more illustrated and calls for an optimistic approach of still more refined materials optimizations.

Acknowledgment. We are very much indebted to IRSIA, CRIF, SOLVAY, and LABOFINA who sponsored this research through a University Interindustry research project. We are also grateful to SPPS for financial support. We thank M. Palumbo and J. Wolter for their helpful technical assistance. The collaboration of LABOFINA for Izod and falling dart measurements and of SOLVAY for transmission electron microscopy examination is greatly appreciated.

Registry No. SAN, 9003-54-7; PS–PMMA (copolymer), 25034-86-0; PB–PMMA (copolymer), 25232-40-0.

References and Notes

(1) Bucknall, C. B. *Toughened Plastics*; Applied Science: London, 1977. Materials Science Series.
(2) Bucknall, C. B. In *Polymer Blends*; Paul, D. R., Newman, S., Ed.; Academic: New York, 1978: Vol. 2, Chapter 14.
(3) Fayt, R.; Jérôme, R.; Teyssié, Ph. *J. Polym. Sci., Polym. Lett. Ed.* **1981**, *19*, 79.
(4) Fayt, R.; Jérôme, R.; Teyssié, Ph. *J. Polym. Sci., Polym. Phys. Ed.* **1981**, *19*, 1269.
(5) Fayt, R.; Jérôme, R.; Teyssié, Ph. *J. Polym. Sci., Polym. Phys. Ed.*, in press.
(6) Fayt, R.; Jérôme, R.; Teyssié, Ph., submitted for publication in *J. Appl. Polym. Sci.*
(7) Teyssié, Ph.; Fayt, R.; Jérôme, R.; Ouhadi, T. European Patent Application No 76539, Solvay Cie, 1982.
(8) Fayt, R.; Jérôme, R.; Teyssié, Ph., submitted for publication in *J. Polym. Sci., Polym. Phys. Ed.*
(9) It has been shown indeed to be the case for stabilized polystyrene–polyethylene blends subjected to injection molding.[8]

Model Copolymerization Reactions. Evidence against Participation of a Donor–Acceptor Complex in Reactions of the 1-Butyl Radical with *N*-Phenylmaleimide and 2-Chloroethyl Vinyl Ether

SHARON A. JONES

Department of Chemistry, Carnegie-Mellon University, Pittsburgh, Pennsylvania 15213

DAVID A. TIRRELL*

Polymer Science and Engineering Department, University of Massachusetts, Amherst, Massachusetts 01003.
Received December 31, 1985

The participation of electron donor–acceptor (EDA) complexes in alternating radical copolymerizations has been debated for nearly 40 years.[1] It has been suggested that some alternating copolymerizations may not be copolymerizations at all but instead may proceed via successive concerted additions of 1:1 comonomer complexes (**2**) to growing polymeric radicals (**1**)

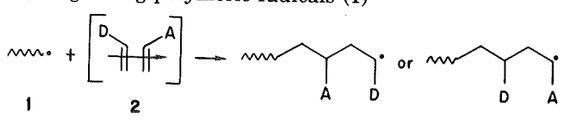

1 **2** (1)

This is an intriguing idea and, if correct, would explain not only the alternating copolymer structure but also certain kinetic features of alternating copolymerization.[2]

0024-9297/86/2219-2080$01.50/0

Table I
Consumption of NPM by Addition of 1-Butyl Radical

reactn	$[BuHgBr]_0$[a]	$[NPM]_0$[d]	$[CEVE]_0$	$[NPM]_f$[e]	$[7]_f$	$\frac{[7]_f}{[NPM]_0 - [NPM]_f}$
1[b]	0.244	0.268	0.278	0.211	0.0547	96 ± 4%[f]
2[c]	0.226	0.248	0.278	0.147	0.106	105 ± 5
3	0.228	0.245	0.307	0.113	0.111	84 ± 10
4	0.165	0.162	0.211	0.002	0.155	97 ± 4
5	0.159	0.151	0.195	0.001	0.145	97 ± 10
6	0.154	0.154	0.182	0.001	0.161	105 ± 2
7	0.156	0.166	0.204	0.001	0.153	93 ± 4

[a] All concentrations are given in moles per liter. [b] Includes injections after 30 min and 3 h. [c] Includes injections after 30 min and 48 h. [d] Initial [NPM]. [e] Final [NPM]. [f] Reported as mean plus or minus one standard deviation for 2–4 determinations.

But do alkyl radicals undergo such concerted additions? Radical trapping experiments may be used to test this idea and to determine the extent to which complex addition competes with simple addition of uncomplexed olefins (eq 2).

$$\begin{aligned} R\cdot &\xrightarrow{A} RA\cdot \xrightarrow{T} \underset{\mathbf{3}}{RAT} \\ &\xrightarrow{D} RD\cdot \xrightarrow{T} \underset{\mathbf{4}}{RDT} \\ &\xrightarrow{AD} RAD\cdot \xrightarrow{T} \underset{\mathbf{5}}{RADT} \\ &\xrightarrow{DA} RDA\cdot \xrightarrow{T} \underset{\mathbf{6}}{RDAT} \end{aligned} \qquad (2)$$

(Here A indicates donor monomer, D indicates acceptor monomer, $\overline{AD}$ indicates complex, and T indicates radical trap.) The radical of interest is generated in the presence of the donor (D) and acceptor (A) monomers, and the resulting adducts are trapped to yield products **3**–**6**. Accurate mass balances for A and D then allow determination of the dominant pathway(s) for monomer consumption.

We have recently reported the use of the "mercury method"[3] in an investigation of the magnitude of penultimate effects in a model styrene–acrylonitrile copolymerization.[4] The needed radicals were generated by hydride reduction of alkyl mercuric halides, and the olefin adducts were trapped by efficient hydrogen atom transfer. The technique is well suited to an investigation of concerted complex addition as outlined in eq 2.

We report in this paper the use of the mercury method to examine the addition of the 1-butyl radical to *N*-phenylmaleimide (NPM) and 2-chloroethyl vinyl ether (CEVE). Olson and Butler reported recently a very careful analysis of the radical copolymerization of NPM and CEVE and suggest that concerted complex addition dominates the chain-growth process.[5–7] This then appears to be an attractive system in which to demonstrate the use of radical trapping techniques in a test of the complex addition hypothesis.

Experimental Section

Preparations. 1-Butylmercuric Bromide (BuHgBr). 1-Butylmercuric bromide was prepared according to the procedure of Slotta and Jacobi.[8]

2-Butyl-*N*-phenylsuccinimide. To a solution of 0.44 g (2.54 mmol) of NPM and 0.57 g (1.69 mmol) of 1-butylmercuric bromide in 5 mL of CH_2Cl_2 was added a solution of 0.128 g (3.38 mmol) of $NaBH_4$ in 0.5 mL of H_2O. When no further evolution of gas was apparent, the mixture was analyzed by gas chromatography (9 ft stainless steel column packed with 3% SE-30 on 80/100 Supelcoport; column temp, 180 °C; He flow, 50 mL/min) to monitor the disappearance of 1-butylmercuric bromide. In two subsequent additions, 0.06 and 0.04 mL of a 6.65 M solution of $NaBH_4$ in H_2O were added to the reaction mixture. After the second addition, no BuHgBr was detected. The solution was then filtered over $MgSO_4$ to remove water. Kugelrohr distillation followed by preparative thin-layer chromatography (3:1 CH_2Cl_2:petroleum ether) yielded 30 mg (10%) of 2-butyl-*N*-phenylsuccinimide, mp 59 °C. ^1H NMR (300 MHz, CD_2Cl_2) δ 0.9 (triplet, 3 H), 1.2–2.0 (broad, 10 H), 2.6 (multiplet, 1 H), 2.9 (multiplet, 1 H). m/e = 231. Anal. Calcd for $C_{14}H_{17}NO_2$: C, 72.7; H, 7.4; N, 6.1. Found: C, 72.2; H, 7.3; N, 5.8.

Monomer Mass Balance Experiments. In a typical reaction 0.0445 g (0.257 mmol) of NPM and 0.0368 g (0.300 mmol) of CEVE were added to 0.078 g (0.231 mmol) of BuHgBr in 0.85 mL of CH_2Cl_2. To this solution at room temperature was added 4.54 mg (0.12 mmol) of $NaBH_4$ in 0.1 mL of H_2O. After 30 min, elemental Hg was separated, and the reaction mixture was analyzed by gas chromatography and gas chromatography/mass spectrometry (GC/MS) (9 ft stainless steel column, 3% SE-30 on 80/100 Supelcoport; column temp, 100 °C for 10 min, programmed to 250 °C; He, 50 mL/min). In some experiments, *tert*-butylbenzene was added as an internal chromatographic standard.

Results and Discussion

Generation of the 1-butyl radical by hydride reduction of 1-butylmercuric bromide in solutions of NPM and CEVE provides predominantly 2-butyl-*N*-phenylsuccinimide (**7**). Table I summarizes the results of seven trapping experiments and compares the yields of **7** with the amounts of NPM consumed. Although there is some fluctuation in the yields of **7**, on average 97 ± 7% of the reacted NPM appears in this product, regardless of the NPM conversion. Within experimental error, NPM is consumed quantitatively by simple radical addition; concerted complex addition is negligible. Furthermore, we are unable to detect by GC/MS the formation of any compounds of m/e 338, which might have been formed by concerted addition of NPM and CEVE.

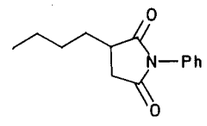

7

These results deserve comment in light of the recent work of Olson and Butler on radical copolymerization of NPM and CEVE.[5–7] On the basis of variations in copolymer ^{13}C NMR spectra with changes in reaction conditions, Olson and Butler suggest that the dominant propagation step in this copolymerization is a concerted addition of a CEVE-terminated macroradical to a 1:1 NPM:CEVE complex. We have repeated the most critical copolymerization experiments of Olson and Butler, and we find them to be readily reproducible. The results in Table I, however, appear inconsistent with the notion that concerted complex addition is the dominant pathway for consumption of NPM in its copolymerization with CEVE.

Might the results in Table I be misleading with regard to the mechanism of the radical copolymerization of NPM